

Thermoelectric Quantum-Dot Superlattices with High ZT

T.C. HARMAN, P.J. TAYLOR, D.L. SPEARS, and M.P. WALSH

Lincoln Laboratory, Massachusetts Institute of Technology, Lexington, MA 02420-9108

Following the experimentally observed Seebeck coefficient enhancement in PbTe quantum wells in $\text{Pb}_{1-x}\text{Eu}_x\text{Te}/\text{PbTe}$ multiple-quantum-well structures which indicated the potential usefulness of low dimensionality, we have investigated the thermoelectric properties of $\text{PbSe}_x\text{Te}_{1-x}/\text{PbTe}$ quantum-dot superlattices for possible improved thermoelectric materials. We have again found enhancements in Seebeck coefficient and thermoelectric figure of merit (ZT) relative to bulk values, which occur through the various physics and materials science phenomena associated with the quantum-dot structures. To date, we have obtained estimated ZT values approximately double the best bulk PbTe values, with estimated ZT as high as about 0.9 at 300 K.

Key words: PbSeTe/PbTe, quantum-dots, thermoelectric figure of merit (ZT)

INTRODUCTION

Whall and Parker¹ first suggested using multilayer systems prepared by molecular beam epitaxy (MBE) for improved thermoelectric materials. Several papers² were presented on thermoelectric superlattices in 1992 including experimental results on PbSeTe/BiSb superlattices by Lincoln Laboratory.³ Reduced dimensional superlattice systems were proposed as a means to greatly enhance the thermoelectric figure of merit (ZT) as a result of the effects of confinement on the electronic density of states.⁴⁻⁶ Subsequently, it was shown that additional effects need to be included in order to obtain a more complete understanding of these complex structures.^{7,8} Recently, there has been an increasing interest in quantum-well and quantum-wire superlattice structures in the search to find improved thermoelectric materials for applications in cooling and power generation.⁹ An earlier experimental investigation of $\text{Pb}_{1-x}\text{Eu}_x\text{Te}/\text{PbTe}$ quantum-well superlattices grown by MBE yielded an enhanced ZT due to the quantum confinement of electrons in the well part of the superlattice structure.^{10,11} Quantum wires have been calculated to have much higher ZTs than quantum wells.⁸ Quantum dots (QDs) may have even higher ZT values than quantum wires.

Quantum dots represent the ultimate in reduced dimensionality, i.e., zero dimensionality. The energy of an electron confined in a small volume by a poten-

tial barrier as in a QD is strongly quantized, i.e., the energy spectrum is discrete. For QDs the conduction band offset and/or strain between the QD and the surrounding material act as the confining potential. The quantization of energy, or alternatively, the reduction of the dimensionality is directly reflected in the dependence of the density of states on energy. For a zero-dimensional system (QD), the density of states (dN/dE) of the confined electrons has the shape of a delta-like function¹²

$$dN/dE \propto \sum_{\epsilon_i} \delta(E - \epsilon_i) \quad (1)$$

where ϵ_i are discrete energy levels and δ is the Dirac function. Thus, an enhanced density of states is a possibility even in partially confined QD superlattice (QDSL) structures. Consequently, an enhancement in the Seebeck coefficient S and the thermoelectric power factor $P = S^2\sigma$ (where σ is the electrical conductivity) may occur for a suitable structure in which the chemical potential lies within a few kT s of the delta-like function of the ground state and/or one of the excited states of the partially confined QDs. In addition, the chemical potential should lie near a suitable band edge of a good thermoelectric material. In real materials, tunneling, thermal and inhomogeneous broadening as well as a weak potential barrier surrounding the QD may contribute to reducing the confinement effect. An enhancement of the Seebeck coefficient and the power factor in the PbSeTe/PbTe QDSL system has been reported.¹³

(Received October 4, 1999; accepted November 10, 1999)

In addition to the possibility of an enhancement in the power factor, another advantage of having a QDSL structure is the enormous density of dissimilar materials interfaces (involving the wetting layer, the matrix or spacer layer, and dot layer of the QDSL structure) which is expected to lower the lattice thermal conductivity to values below those attainable by merely alloying.¹⁴ Experimental results on the reduction of the thermal conductivity of superlattices have been reported in which the values were much lower than that of their constituents and even smaller than the thermal conductivity value of the equivalent compositional alloys.¹⁵ The possibility of phonon engineering combined with power-factor engineering may result in large improvements in the ZT of already good thermoelectric materials.

A significant lattice mismatch is needed in order for

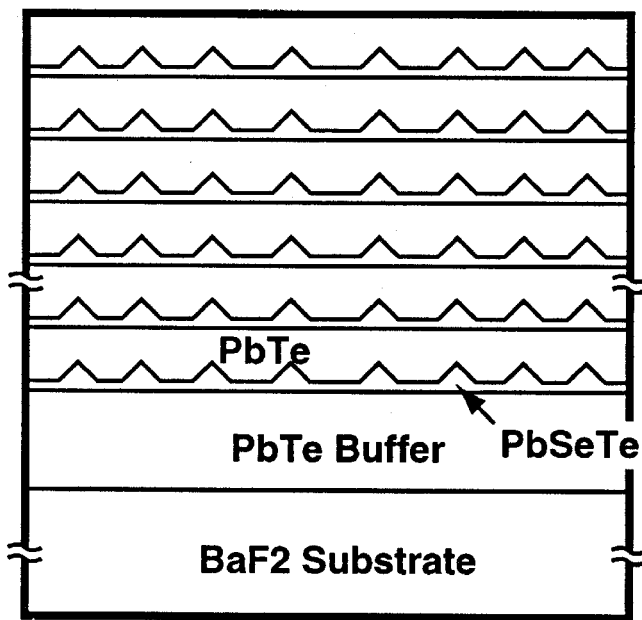


Fig. 1. Schematic cross section of the quantum-dot superlattice structure investigated.

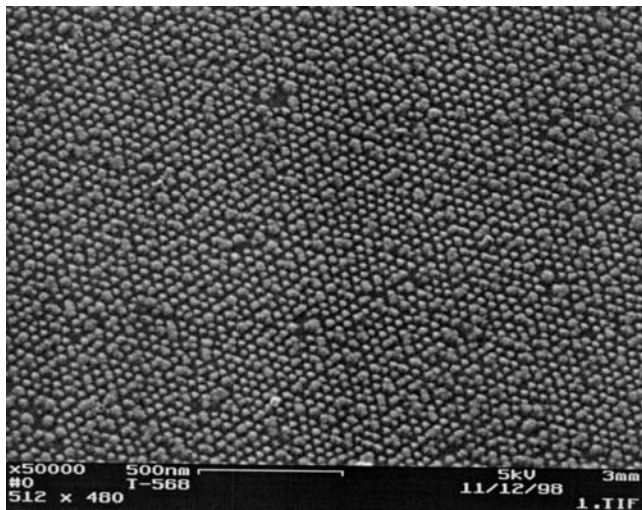


Fig. 2. Field-emission SEM image of quantum-dot superlattice structure.

islands or dots to form. A good thermoelectric material is needed in order to start with a reasonably high ZT. It is conjectured that a high static dielectric constant is needed not only to suppress impurity scattering of the electron carriers but also to minimize interface scattering of the carriers. ZT increases as the lattice thermal conductivity decreases for constant temperature, power factor, and electronic part of the total thermal conductivity. Upon considering the above criteria, the PbSeTe/PbTe superlattice system appears to be a very good model system for investigation of thermoelectric QDSL phenomena.

As a first step to realizing large improvements in the ZT of a QDSL thermoelectric material, we report on the growth and characterization of QDSL structures composed of $\text{PbSe}_{0.98}\text{Te}_{0.02}$ QDs and PbTe matrix layers. Please note that QDs have already been reported for a PbSe deposit on a PbTe surface¹⁶ and for a 60-period PbSe/PbEuTe QDSL structure.^{17,18} The islands or QDs form in order to reduce the large heteroepitaxial free energy component and allow the strain in the $\text{PbSe}_{0.98}\text{Te}_{0.02}$ to partially relax. The islanding process reduces the interface energy by limiting the contact of the $\text{PbSe}_{0.98}\text{Te}_{0.02}$ with the PbTe surface upon which it is grown, and allows the $\text{PbSe}_{0.98}\text{Te}_{0.02}$ free surface to at least partially relax. The strain-induced islanding technique produces the QDs and is called the Stranski-Krastanow epitaxial growth method. When enveloped by PbTe matrix material, these islands may possibly be used to partially confine the electrons in the QDs.

For the experimental realization of a large number of QDs with good quality (high degree of ordering), optimal separational distance, and nearly uniform dot size, we use MBE, which is noted for atom-layer by atom-layer control, reproducibility, and flexibility. Another advantage of MBE-grown Pb-salt structures is that the sticking coefficients of well-known MBE growth chamber contaminants are unusually low.¹⁹

RESULTS AND DISCUSSION

The MBE growth was carried out in a modified 360-type (T-series) growth chamber with an associated custom-built load-lock chamber as described previously.²⁰ The effusion cells on the cell flange used for the growth of PbSeTe/PbTe superlattice structures contained PbTe, PbSe, BiSb or Bi_2Te_3 , and Te. The MBE substrate holder accommodated BaF_2 substrates with 18×18 -mm square shape. A 30-keV RHEED system (used at 12 keV) was employed during film growth to optimize and monitor the deposition. Alternating RHEED streaks and chevron-shaped dots were observed throughout the growth runs of the QDSL structures. Molecular and atomic beam fluxes arriving at the substrate location were monitored via the beam-flux ion gauge. The main flux measurement was a nude Bayard-Alpert gauge, mounted on a manipulator, so that it could be rotated into the substrate position. In this position, the beams from the individual sources can be monitored and calibrated. Precise run-to-run control of composition requires pre-

cise knowledge of the PbTe, PbSe and Te beam fluxes. The beam flux of the n-type dopant source (BiSb or Bi₂Te₃) was adjusted and monitored by measuring the Hall coefficient of grown films by the van der Pauw method. The typical growth rate was 0.8 μm/h to 1.4 μm/h. The carrier concentration of the calibration PbTe and PbSe_{0.98}Te_{0.02} growth runs and the PbSe_{0.98}Te_{0.02}/PbTe superlattice structures were calculated from the Hall coefficient. For the growth of the PbSe_{0.98}Te_{0.02}/PbTe superlattice structures, the BiSb or Bi₂Te₃, and Te shutters were open during the entire growth run, whereas the PbTe and PbSe shutters were alternately opened and closed. A schematic cross section of a PbSe_{0.98}Te_{0.02}/PbTe superlattice structure along with the approximately 200-nm-thick Bi-doped PbTe buffer layer and the (111) BaF₂ substrate is shown in Fig. 1. After the growth of a 0.6- to 0.7-nm-thick wetting layer, PbSe_{0.98}Te_{0.02} spontaneously grows in the form of QDs. The PbTe grows to replanarize the surface. This behavior automatically repeats itself for over 600 periods in these test structures.

It is well known that lead chalcogenides can be doped by varying the Pb-to-chalcogenide ratio, but this is not the best way to dope the material. Lead vacancies can dope the material p-type whereas chalcogenide vacancies can dope the material n-type. However, the vacancy dopant mechanism yields maximum carrier concentrations of about $1 \times 10^{18} \text{ cm}^{-3}$ in our MBE system using thermally evaporated PbSe_{0.98}Te_{0.02} and PbTe material because of the low growth temperature (300°C to 330°C, as determined by infrared pyrometry) whereas the optimum carrier concentration for a good Pb-chalcogenide thermoelectric material is $6 \times 10^{18} \text{ cm}^{-3}$ or higher at 300 K. Thus, an impurity must be used for doping. Years ago at Lincoln Laboratory, the dopant behavior (carrier type) of eleven impurity elements in bulk PbTe was investigated by the Bridgman growth technique and various post-growth annealing processes^{21,22} and their thermoelectric power factors were determined.²³ It turned out that Bi yielded the highest thermoelectric power factors among the dopants investigated.

The field-emission scanning electron microscope (FE-SEM) image (i.e., at 50,000 X magnification) in Fig. 2 shows the QDs after growth of the 240th PbSe_{0.98}Te_{0.02} wetting and dot layer and without the 240th PbTe replanarization layer. The film was rapidly cooled to room temperature to preserve this epitaxial surface structure. The white images are the individual QDs in the planar array. There are approximately 9×10^{10} quantum dots/cm² in this last or surface layer of the superlattice. Atomic force microscopy images also show that the height-to-base aspect ratio of about 1:3 is much larger than for other materials systems, and their narrow size distribution is much narrower than that of QDs observed in other materials systems.

The Seebeck coefficient vs. carrier concentration is shown in Fig. 3. Data for the best bulk PbTe, the PbTe/Te superlattice, and the new QDSL structures are given. Our data indicate that the Seebeck coefficient

of the best bulk PbSe follows the same curve as the PbTe and may be described by the following empirical Seebeck coefficient vs. carrier concentration n relationship,¹¹ i.e.,

$$S (\mu\text{V/K}) = -477 + 175 \log_{10} (n/10^{17} \text{ cm}^{-3}) \quad (2)$$

Currently, the most plausible explanation for the Seebeck coefficient enhancement for the PbTe/Te data shown in Fig. 3 appears to be that the effective scattering parameter r is increased as a result of extra scattering introduced by the extra Te adsorbed periodically in the PbTe lattice.^{20,24} The increased Seebeck coefficient enhancement for the QDSL structure is believed a consequence of quantum effects from the reduced dimensionality of partially confined electrons in the PbSe_{0.98}Te_{0.02} QDs as well as a more favorable scattering mechanism. The Seebeck coefficient

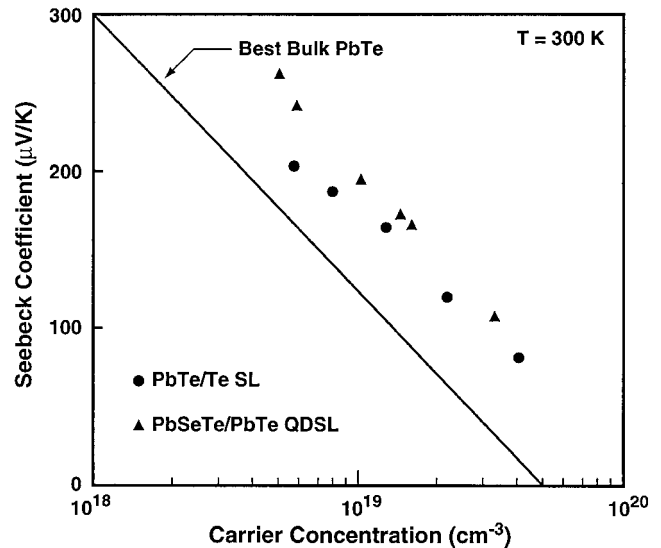


Fig. 3. Seebeck coefficient vs. carrier concentration for n-type PbTe-based structures.

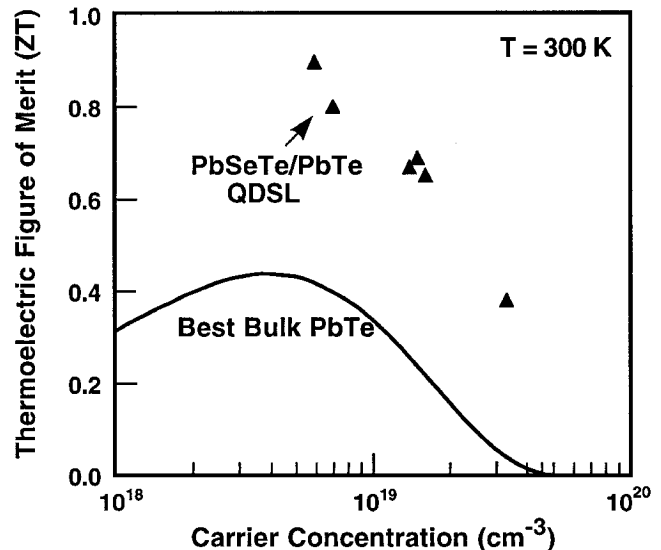


Fig. 4 Thermoelectric figure of merit vs. carrier concentration for bulk PbTe and the new PbSeTe/PbTe quantum-dot superlattice structures.

coefficients of all $\text{PbSe}_{0.98}\text{Te}_{0.02}/\text{PbTe}$ samples in Fig. 3 are much greater than the values calculated from the S vs. n relationship of Eq. 2.

The thermoelectric figure of merit versus carrier concentration at 300 K is shown in Fig. 4 for QDSL samples as well as for bulk PbTe. The solid curve for bulk PbTe was obtained from the power factor using thermal conductivity values calculated from the literature lattice thermal conductivity along with the Weidemann-Franz law as described in Ref. 11. The solid curve provides information near the optimum bulk carrier concentration where $ZT = 0.45$. ZT values for the QDSL samples are much higher (for the same carrier concentration) than either bulk or homogeneous film PbTe or PbTe/Te. These ZT values were obtained from the measured Seebeck coefficient and electrical resistivity values along with calculated thermal conductivity values. The calculated thermal conductivity values are based on the Wiedemann-Franz law and published experimentally derived values of the lattice thermal conductivity κ_l for the mean or equivalent alloy composition of the QDSL samples. It is well known that $\text{PbSe}_{0.5}\text{Te}_{0.5}$ has a much lower lattice thermal conductivity²⁵ than either PbTe or PbSe at 300 K by a factor of 2 to 2.5. We determined the equivalent alloy compositions of each sample by two independent methods, i.e., from x-ray diffraction and growth parameters. However, recent experimental results²⁶ on the lattice thermal conductivity of Si/Ge superlattice structures (a 4.2% lattice-mismatched system) would suggest that the above estimates for the lattice thermal conductivity of $\text{PbSe}_x\text{Te}_{1-x}/\text{PbTe}$ (a 5.2% lattice mismatched system) superlattice films are too high. To be conservative, we used the values from Ref. 25 measured on bulk alloys of PbSeTe alloys in our estimates of ZT shown in Fig. 4. Nevertheless, we found some very high ZT s in these $\text{PbSe}_{0.98}\text{Te}_{0.02}/\text{PbTe}$ superlattice samples of up to about 0.9 at 300 K. Thus, these MBE-grown $\text{PbSe}_{0.98}\text{Te}_{0.02}/\text{PbTe}$ quantum dot superlattice samples have shown significantly enhanced Seebeck coefficients, power factors and ZT s.

SUMMARY

Large increases in Seebeck coefficient, power factor and ZT have been measured in $\text{PbSeTe}/\text{PbTe}$ QDSLs. The improvement in ZT is attributed to the following: (1) a more favorable carrier scattering mechanism due to adsorbed or precipitated extra Te, (2) the presence of $\text{PbSe}_{0.98}\text{Te}_{0.02}$ islands or dots imbedded in a PbTe matrix and believed to result in partial confinement of electrons in the QDs, and (3) the lowering of the lattice thermal conductivity to at least the values of the homogeneous pseudobinary $\text{PbSe}_x\text{Te}_{1-x}$ alloys. Experimental values for the Pb-chalcogenide film in-plane room-temperature ZT values have been increased from approximately 0.52 for PbTe/Te structures to about 0.9 for $\text{PbSe}_{0.98}\text{Te}_{0.02}/\text{PbTe}$ QDSL structures. Further improvements in the ZT are anticipated based on the potential for lowering the lattice thermal conductivity because of the enormous num-

ber of dissimilar materials interfaces present in QDSL structures and with periods in the 10 to 15-nm range. Also, many variables need to be optimized including alloying with other compounds.

ACKNOWLEDGEMENTS

This work was sponsored by the Defense Advanced Projects Research Agency (DARPA), the Department of the Navy and the Army Research Office under Air Force Contract No. F19628-95-C-0002. The opinions, interpretations, conclusions, and recommendations are those of the author(s) and are not necessarily endorsed by the United States Air Force.

REFERENCES

1. T.E. Whall and E.H. C. Parker, *Proc. First European Conf. on Thermoelectrics*, ed. D.M. Rowe (London: Peter Peregrinus Ltd., 1987), pp. 51–63.
2. S.B. Horn, *Proc. of the 1st National Thermogenic Cooler Conf.* (Fort Belvoir, VA: Center for Night Vision and Electro-Optics, 1992).
3. T.C. Harman, U.S. patent 5,415,699 (May 16, 1995); U.S. patent 5,900,071 (May 4, 1999).
4. L.D. Hicks and M.S. Dresselhaus, *Phys. Rev. B* 47, 12727 (1993).
5. L.D. Hicks, T.C. Harman, and M.S. Dresselhaus, *Appl. Phys. Lett.* 63, 3230 (1993).
6. L.D. Hicks and M.S. Dresselhaus, *Phys. Rev. B* 47, 16631 (1993).
7. J.O. Sofo and G.D. Mahan, *Appl. Phys. Lett.* 65, 2690 (1994).
8. D.A. Broido and T.L. Reinecke, *Phys. Rev. B* 51, 13797 (1995); T.L. Reinecke and D.A. Broido, *Proc. of the XVI Int. Conf. on Thermoelectrics* (Piscataway, NJ: IEEE, 1997), p. 424.
9. G. Mahan, B. Sales, and J. Sharp, *Phys. Today* 50, 42 (1997).
10. L.D. Hicks, T.C. Harman, X. Sun, and M.S. Dresselhaus, *Phys. Rev. B* 52, R10493 (1996).
11. T.C. Harman, D.L. Spears, and M.J. Manfra, *J. Electron. Mater.* 25, 1121 (1996).
12. See for example, L. Jacak, P. Hawrylak, and A. Wojs, *Quantum Dots* (Berlin - Heidelberg - New York: Springer-Verlag, 1998), p. 16.
13. T.C. Harman, P.J. Taylor, M.P. Walsh, and D.L. Spears, Abstract for the 41st Electron. Mater. Conf., Santa Barbara, CA, June 30–July 2, 1999, *J. Electron. Mater.* 28, 54 (1999).
14. G. Chen and M. Neagu, *Appl. Phys. Lett.* 71, 2761 (1997).
15. See T. Borca-Tasciuc, D. Song, J.L. Liu, G. Chen, K.L. Wang, X. Sun, M.S. Dresselhaus, T. Radetic, and R. Gronsky, *Thermoelectric Materials 1998*, ed. T.M. Tritt et al. (Warrendale, PA: MRS, 1999), p. 473 and references therein.
16. M. Pinczoliths, G. Springholz, and G. Bauer, *Appl. Phys. Lett.* 73, 250 (1998).
17. G. Springholz, V. Holy, M. Pinczoliths, and G. Bauer, *Science* 282, 734 (1998).
18. V. Holy, G. Springholz, M. Pinczoliths, and G. Bauer, *Phys. Rev. Lett.* 83, 356 (1999).
19. N. Frank, A. Voiticek, H. Clemens, A. Holzinger, and G. Bauer, *J. Cryst. Growth* 126, 293 (1993).
20. T.C. Harman, D.L. Spears, and M.P. Walsh, *J. Electron. Mater.* 28, L1 (1999).
21. A.J. Strauss, personal communication.
22. A.J. Strauss, *J. Electron. Mater.* 2, 553 (1973).
23. T.C. Harman, unpublished.
24. T. Koga, T.C. Harman, X. Sun, S.B. Cronin, and M.S. Dresselhaus, *Thermoelectric Materials 1998*, ed. T.M. Tritt et al. (Warrendale, PA: MRS, 1999).
25. E.D. Devyatkova and V.V. Tikhonov, *Sov. Phys.-Solid State* 7, 1427 (1965) and references therein.
26. S.M. Lee, D.G. Cahill, and R. Venkatasubramanian, *Appl. Phys. Lett.* 70, 2957 (1997).